

Piezocomposite Actuator Arrays for Correcting and Controlling Wavefront Error in Reflectors

Samuel Case Bradford*, Lee D Peterson†, Catherine M Ohara‡, Fang Shi‡,
Greg S Agnes*, Samuel M Hoffman*

Jet Propulsion Laboratory, California Institute of Technology, Pasadena CA 91109

William Keats Wilkie§

NASA Langley Research Center, Hampton VA 23681

Three reflectors have been developed and tested to assess the performance of a distributed network of piezocomposite actuators for correcting thermal deformations and total wavefront error. The primary testbed article is an active composite reflector, composed of a spherically curved panel with a graphite face sheet and aluminum honeycomb core composite, and then augmented with a network of 90 distributed piezoelectric composite actuators. The piezoelectric actuator system may be used for correcting as-built residual shape errors, and for controlling low-order, thermally-induced quasi-static distortions of the panel. In this study, thermally-induced surface deformations of 1 to 5 microns were deliberately introduced onto the reflector, then measured using a speckle holography interferometer system. The reflector surface figure was subsequently corrected to a tolerance of 50 nm using the actuators embedded in the reflector's back face sheet. Two additional test articles were constructed: a borosilicate flat window at 150 mm diameter with 18 actuators bonded to the back surface; and a direct metal laser sintered reflector with spherical curvature, 230 mm diameter, and 12 actuators bonded to the back surface. In the case of the glass reflector, absolute measurements were performed with an interferometer and the absolute surface was corrected. These test articles were evaluated to determine their absolute surface control capabilities, as well as to assess a multiphysics modeling effort developed under this program for the prediction of active reflector response. This paper will describe the design, construction, and testing of active reflector systems under thermal loads, and subsequent correction of surface shape via distributed piezoelectric actuation.

Introduction

As part of an ongoing Jet Propulsion Laboratory internal R&TD activity, this report investigates active piezocomposite systems as a less costly, lightweight alternative for future missions needing high surface precision reflectors operating in highly variable thermal environments (e.g., MEO or precessing orbits). Specifically, we developed an innovative active piezoelectric composite reflector system capable of autonomously reacting to variations in thermal environment to maintain precise overall closed-loop shape stability and surface tolerances to within 1 micron per meter of characteristic length.^{1,2}

Our primary concept consists of a lightweight, relatively compliant, high surface precision composite reflector (Figure 1) with a latticework of flat piezoelectric composite actuators (Figure 2) integrated with the backing face sheet. Lightweighting the composite panel structure increases susceptibility to low-order thermal distortion and warping, but this is compensated actively through closed loop control of the actuator lattice. The driving motivation of this research was to develop lightweight composite reflectors for microwave applications, with surface figure requirements of 10 micron RMS over meter-scale and larger reflectors.

*Advanced Deployable Structures Group, Jet Propulsion Laboratory

†Mechanical Systems Engineering Division, Jet Propulsion Laboratory

‡Active Optics Group, Jet Propulsion Laboratory

§Branch Head, Structural Dynamics, NASA Langley Research Center

Large, precision composite reflectors for spaceflight can be relatively massive and expensive to fabricate. Typically, a heavy reflector structure is necessary to maintain tight reflector surface tolerances and overall shape under highly variable mission thermal orbital environments. Concepts for the Scanning Microwave Limb Sounder (SMLS, Figure 3) composite primary reflector, for example, are over 4 meters long, and weigh as much as the entire remainder of the instrument and spacecraft. An active reflector could provide a lighter-weight, lower-cost alternative to a purely passive system.

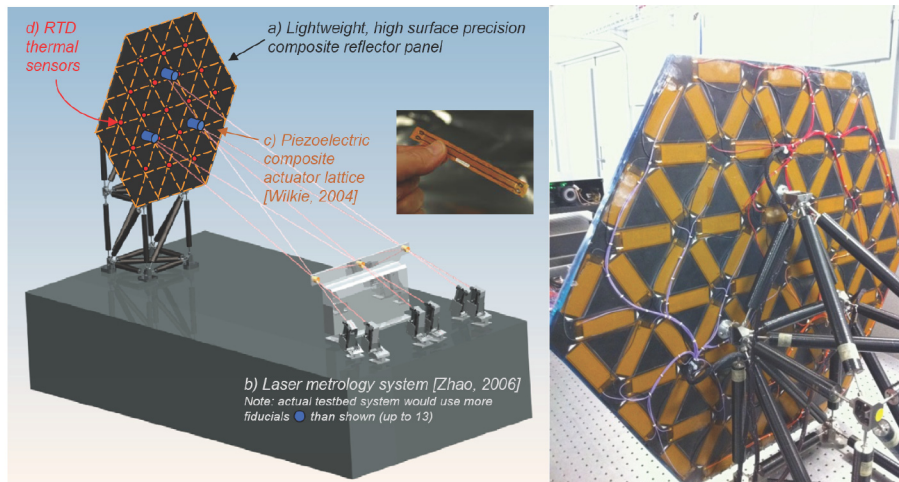


Figure 1: Active Composite Reflector Testbed. At left, low spatial frequency quasistatic thermal distortions of a lightweight reflector panel (a) are measured using a laser metrology system (b). A lattice of piezoelectric composite actuators (c) embedded in the panel back facesheet, is commanded to counteract the distortion. The actuators function much like flat, flexible piezoelectric stacks. Closed-loop control is accomplished through laser metrology feedback, or through an array of calibrated RTD sensors (d). At right, the Active Composite Reflector panel in the Precision Environmental Test Enclosure at JPL. The reflector has 90 individually-addressable actuators that can be driven through a breakout panel or switching unit. Three kinematic magnet mounts attach the panel to the backing truss structure, which is a carbon-fiber truss with titanium end caps bolted into titanium nodes.

As the actuator implementations in this study were able to achieve better than single-micron RMS surface figure control across the meter-scale active composite reflector panel, the research team constructed two additional bench-scale demonstration articles to investigate the scaling laws and control authority at sub-micron surface requirements. The first bench-scale reflector is 23 cm, constructed out of thin polished metal through laser sintering, and then fitted with 12 actuators on the back face. The second bench-scale reflector was constructed from a piece of optical-grade borosilicate glass, 15 cm in diameter, and fitted with 18 actuators on the back face.

Active composite structural concepts have been studied for more than a decade, although functional examples of integrated controlled opto-mechanical systems are rare and no large spaceflight examples exist. Recent developments in NASA spaceflight capable piezoelectric composite actuators^{3,5} and advanced space-qualifiable laser metrology systems,⁷ will allow practical, closed loop active composite reflector systems to be constructed with performance characteristics superior to purely passive reflector designs. Ultimately, this capability can provide a low cost option for missions requiring moderate to large aperture, high precision spaceborne reflectors, and enable science missions requiring precision large apertures with more demanding thermo-structural stability characteristics.

Approach

A preliminary trade study was performed using a Hedgepeth-based⁸ mathematical approach to develop appropriate active composite reflector scaling parameters, and to compare performance with comparable, purely passive (non-active) structural systems. The primary performance metric is overall system mass (which, for active reflectors, will include ancillary power electronics and metrology systems). In parallel, we developed an

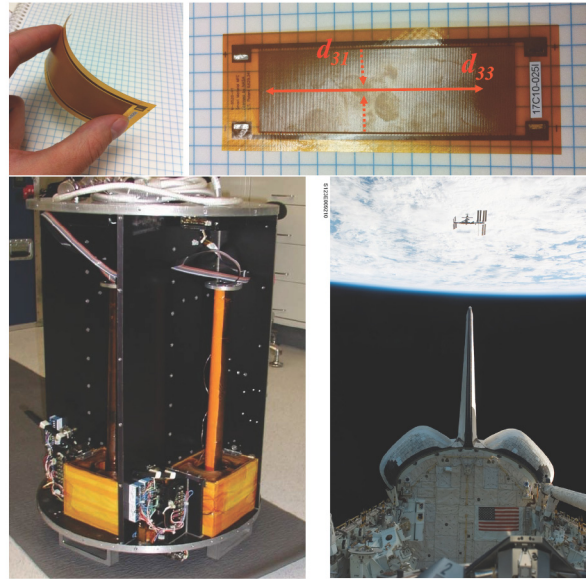


Figure 2: The active composite reflector described here utilizes Macro Fiber Composite piezoelectric actuators (MFC). MFCs are a type of piezoelectric composite actuator,³ functioning much like a flat, flexible, piezoelectric stack (top row). In March 2008 on STS-123,⁴ MFC actuators were flown as a component of the RIGEX⁵ flight experiment (bottom row). MFC actuators are available in several sizes, as well as in custom layouts, and have been incorporated into several testbed panels at JPL.

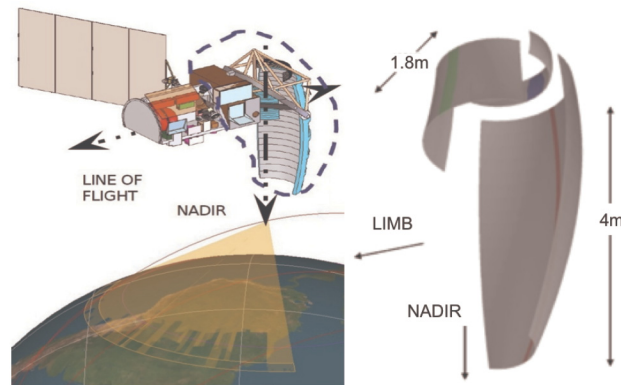


Figure 3: Scanning Microwave Limb Sounder instrument concept with very large composite primary reflector.⁶ The primary reflector for this SMLS concept would be approximately 4 m long and requires surface shape tolerances of better than 12 microns RMS. Achieving this level of surface stability currently requires a comparatively heavy, and expensive, composite structure. A lighter weight, yet correctable, surface figure reflector using the approach outlined in this report is investigated as an alternative.

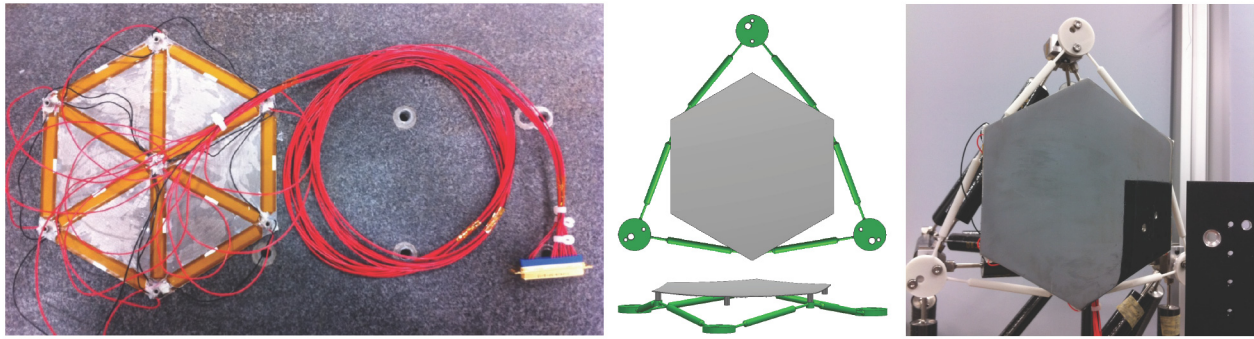


Figure 4: Solid metal reflector with spherical curvature, 23 cm diameter (point-to-point) and a focal length of 57.5 cm. Thinner actuators were used to give a spoke pattern, with twelve total actuators bonded to the back surface (at left). The front face is polished, and the back face has mount points to a bipod system that supports the reflector on an optical bench or integrated to the Active Composite Reflector testbed support structure.

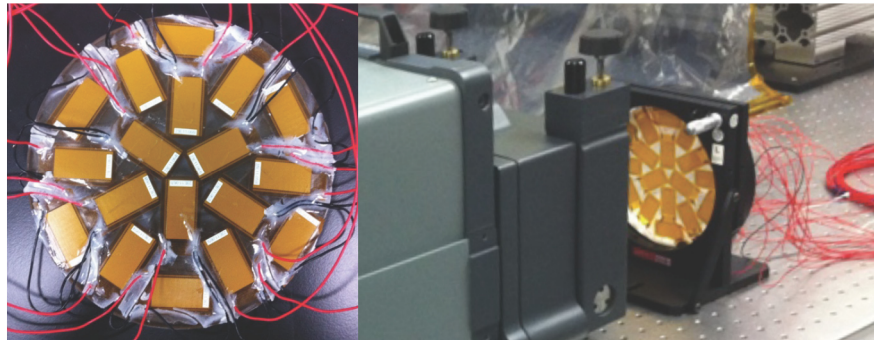


Figure 5: At left, 15 cm borosilicate glass window with 18 actuators bonded to the back surface. Right, the glass surface is suitable for optical testing using an interferometer to measure absolute shape (instead of the relative surface deformations of the speckle holography interferometer used for the larger reflectors in this study).

analytical modeling framework for detailed active composite reflector design and coupled-physics simulations incorporating structural, thermal, and electrical actuation behavior. We used the COMSOL Multiphysics⁹ and SIERRA Multiphysics¹⁰ tools for this task. To support the concept development the team designed, constructed, and tested three active piezocomposite reflector test articles.

A cartoon and photo of the primary reflector testbed is shown in Figure 1. Testing of this demonstration system was performed in the JPL Advanced Large Precision Structures Laboratory test enclosure.¹¹ The facility provides thermal stability (< 0.01 deg C per hr), mechanical vibration isolation (< 0.0001 g rms), and acoustic stability (< 50 dBA) for precision testing. The test campaign for the active reflector began by measuring influence functions for each individually-addressable actuator, and inverting the influence function matrix to generate closed-loop quasistatic thermal distortion correction controllers. The performance and robustness of controllers using feedback from the laser metrology system and other metrology sources were also investigated. Finally, the experimental phase concluded with a distortion compensation demonstration under an applied, slowly varying radiant thermal load. Surface flatness was corrected to better than 50 nm RMS over the 1 m panel.

A metal reflector (Figure 4) was constructed through direct metal laser sintering to obtain a polished metal surface. A sparse actuator geometry was selected, with long narrow actuators, to assess the effects of printthrough of the actuators. Using this sparse actuator array, simple deformations can be imposed on the surface, though not at the spatial frequency required to correct thermal deformations. The third reflector (Figure 5) was constructed by bonding a layer of actuators onto the back of an optical-grade borosilicate window (150 mm). This glass window was suitable for absolute surface shape measurements using a Zygo

interferometer, and had surface errors of 4 waves RMS and 17 waves peak-to-valley before actuation (largely dominated by focus). After actuation the surface shape was better than 2 waves RMS and 10 waves peak-to-valley. This actuation strategy can be used to impose deformations onto the reflector at a very fine scale, correcting for both as-built and thermally-induced deformations.

Panel Construction

The actuators for the composite reflector were trimmed to fit into an isogrid array without overlapping with neighboring actuators or the panel mount points. Bonding operations were split into three phases, one for each lane of actuators in the array (i.e., the 0° , $+60^\circ$ and -60° lanes). A two-part epoxy was applied to each lane of actuators and then cured overnight under pressure. Once the actuators were bonded to the panel, wire leads were soldered to the actuators and brought out to a connector cable, one for each third of the panel.

The metal reflector and glass reflector were both bonded using the same technique, but with the actuators wired to a common signal of +50 V. The actuators are therefore in tension while unpowered, and when operated around 50 V have very linear behavior. Actuators are spaced in an isogrid on the metal reflector, and in an uneven radial pattern (with 120° symmetry) for the glass reflector.

Actuator power can be applied either through a breakout box with terminal attachment points, or by wiring the panel cables into a switch unit or other D/A control system. Each actuator is individually addressable, though if desired they can be operated in zones for coarse control.



Figure 6: MFC actuators during bonding to the back facesheet of the 0.8 m honeycomb panel. Construction was completed in three stages, each lane of actuators (0 , $+60$, -60) was individually bonded to the panel and then cured for 24 hours. Vacuum bagging (right) was used to create an effective bond.

Wavefront Control

Results for all three actuators show very favorable actuator authority for correcting thermally-induced deformations. The meter-scale Active Composite Reflector has been tested most extensively, with a D/A system driven by a 100 V DC power supply. The actuators have an operating range of -500 to +1500 V and are largely linear. Larger voltages can be applied either through a high-voltage D/A system, or by dividing actuators into zones and driving each one with an individual high-voltage power supply.

Correcting thermal deformations in this study required influence functions for each actuator. Actuator influence functions were measured using automated switching software that applied a set voltage to each actuator and measured the surface response. The ensemble of influence functions was then reshaped into an influence matrix suitable for inverting into a sensitivity matrix. Multiplying a desired surface deformation by the sensitivity matrix gives the command voltage profile that will minimize (in a least-squares sense) the residual error between the commanded and measured profile.

A modeled wavefront, \vec{w} , can be expressed as the product of the sensitivity matrix, $\frac{\vec{dw}}{d\vec{u}}$ and a set pattern of input voltages, \vec{u} , e.g.,:

$$\vec{w} = \begin{bmatrix} \frac{d\vec{w}}{d\vec{u}} \end{bmatrix} \vec{u} \quad (1)$$

To solve for the pattern of input voltages, inverting Equation 1 gives:

$$\vec{u} = \begin{bmatrix} \frac{d\vec{w}}{d\vec{u}} \end{bmatrix}^{-1} \vec{w} \quad (2)$$

In the testbed, the calculated voltages are applied back onto the actuators, and the system can operate in a closed-loop to continuously correct the observed surface.

Active Composite Reflector Results

The meter-scale composite reflector has been the primary testbed for developing the actuation strategy and thermal distortion compensation. A sample deformation profile from an applied thermal gradient (Figure 7) is shown in Figure 8. At left, the deformed shape was used as the desired deformation surface (\vec{w}) to generate the voltage profile (\vec{u}) to command for correcting the deformations, as in Equation 2. The voltage profile matches the character of the observed deformations, but in the opposite direction in order to counteract the deformed shape. Residuals (Figure 8, right) are dominated by high spatial frequency printthrough effects, with rescaled residuals presented in Figure 9.

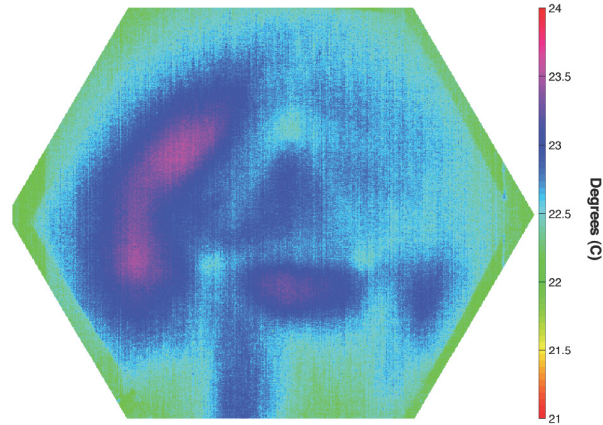


Figure 7: Thermal gradient of 1 C, sample measured during thermal testing in the PETE chamber. The temperature profile across the reflector panel in response to thermal loads shows shadowing from the truss mounting system. Gradients of several degrees C impose deformations of several microns on the front face of the reflector

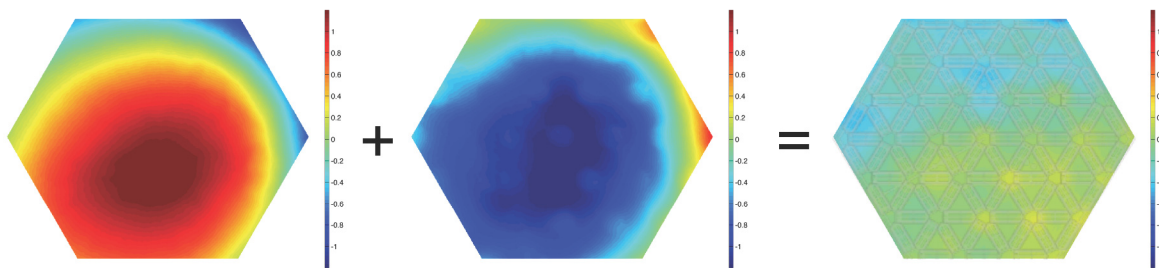


Figure 8: Surface deformations [microns], out-of-plane, induced by a thermal gradient of 1 C. The induced thermal gradient (left) is corrected, open loop by applying a actuation voltages to counteract the observed deformations (center). The difference (right) is dominated by printthrough effects of the actuator pattern, the actuator template is indicated in shaded grey. Several features in the residual correspond to voids in the actuator layout (cf. Figure 1). See Figure 9 for rescaled residuals.

Under closed-loop control, the actuator can correct and then maintain the wavefront of the surface. A heat load was applied to the reflector, with the actuators unpowered, and the surface deformation was allowed to reach a quasi-steady state over several minutes. The actuators were able to correct the thermal deformation, and also continue updating to counteract further deformations in the reflector. Any errors or noise in the influence functions propagate through the control law, the effective noise floor was in the 20-200 nm range depending on the deformation amplitudes reached. The closed-loop results are able to

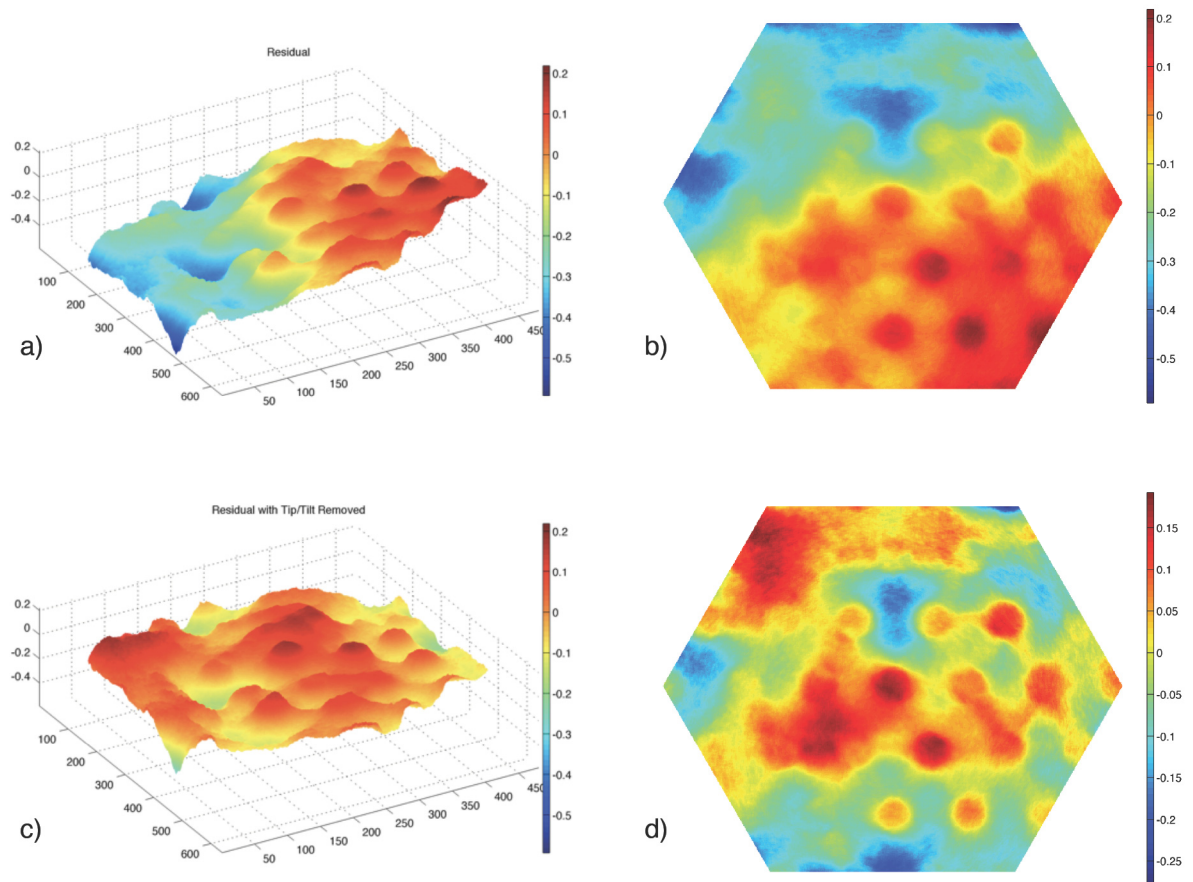


Figure 9: Residuals from open-loop control of active composite reflector. In subfigures a) & b), the residual is dominated by a global tilt term. In subfigures c) & d), the tip and tilt terms have been subtracted, and the remaining residual is dominated by printthrough effects from the actuator layout. Color axes are common between a), b) and c). Subfigure d) has been rescaled for clarity.

correct approximately 90% of a given thermal deformation, across a range of disturbance levels from 0.2 to 2 microns RMS. Control results were obtained using a 100 V D/A unit, which limits the actuators to only 5% of their nominal range. Typical cadence of a control cycle is to measure the current deformation and then calculate a voltage profile that will correct the surface. In Figure 10 the successive iterations show the largest improvement in the first cycle, and successive iterations fine-tune the surface. Figure 11 illustrates two iterations of a control cycle, with the target surface and residuals at each pass.

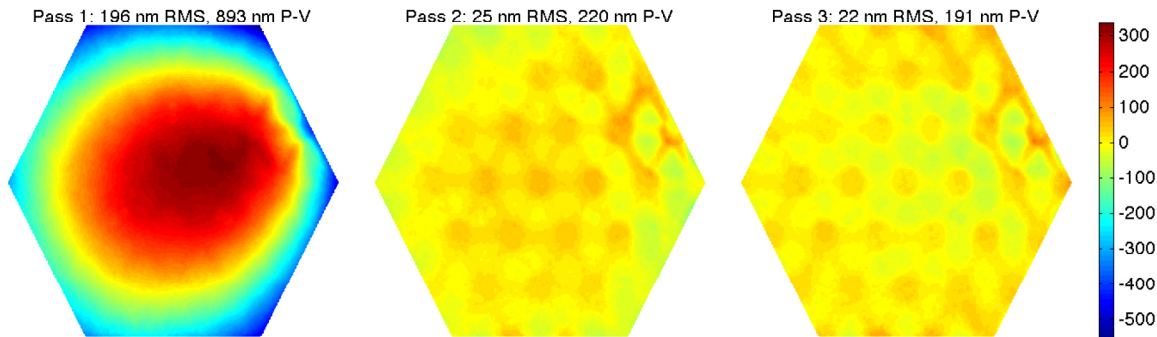
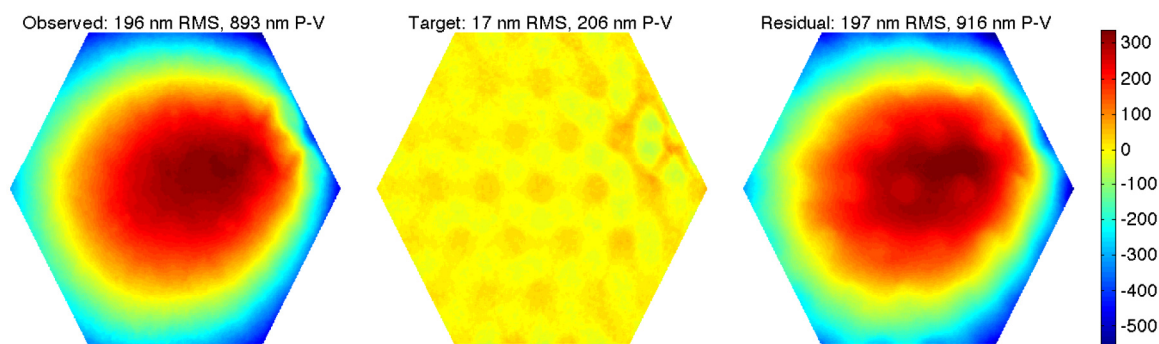
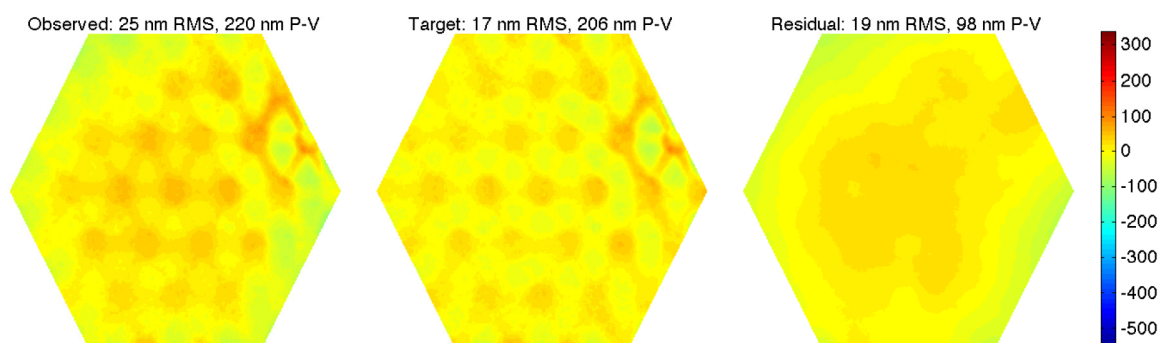


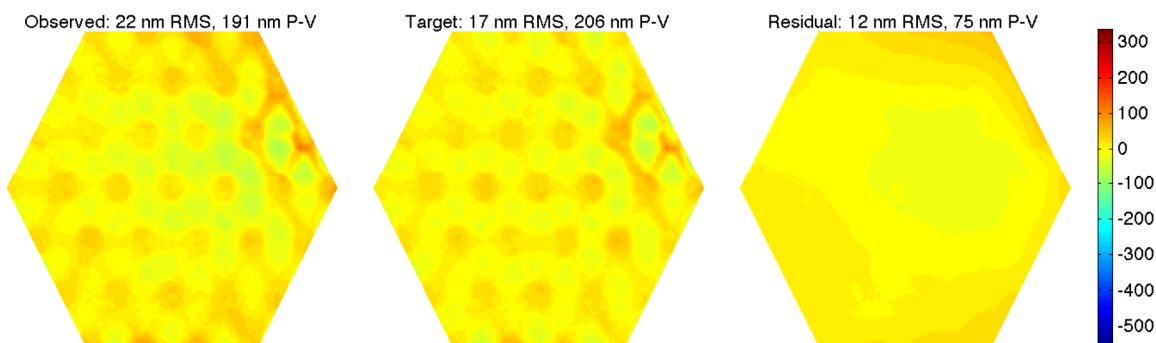
Figure 10: Closed-loop control of Active Composite Reflector under thermal loads. Two passes of the control loop show. The actuator was heated to induce thermal deformations, then the control cycle was initiated at a cadence of every 30 s. The thermal deformations are greatly reduced in the first pass, and successive passes fine-tune the residual as well as correct for thermal deformation induced between control passes.



(a) PASS 0 - Observed deformation, calculated best flat, and residuals. The best flat target surface has very low amplitude printthrough effects from the actuator spacing. With a revised actuator layout the printthrough effects could be minimized.



(b) PASS 1 - After one iteration the surface is greatly improved. High spatial frequency printthrough effects dominate the observed surface, and the residual against the target has some printthrough effects due to the spacing of the actuators.



(c) PASS 2 - The residual between the observed surface and the target is of very low spatial frequency. Printthrough is still visible in the observed shape, though the RMS has been reduced nearly 90% from the original thermally-induced deformation. The misfit is now dominated by low-spatial-frequency errors in influence functions, drift in the metrology system, and continued heating of the reflector. Surface quality for further iterations remains unchanged.

Figure 11: Closed-loop control of Active Composite Reflector under thermal loads. A micron-scale thermal deformation was applied to the reflector, and the surface is corrected in successive iterations at 100 s intervals. Results from two passes are shown, with the forward difference between the observed surface and the target surface. The largest change is in the initial pass.

Active Composite Reflector Model Development

A key component of this research task has been to develop a multiphysics finite-element modeling framework. Figure 12 shows the wavefront error sag for a gravity load along the axis of the mirror. Figure 13) shows the reflector subjected to uniform actuation across all actuators, and in Figure 14 the wavefront difference for selected individual actuators. A full model of the reflector will be key to developing reflector concepts of arbitrary geometries and actuator densities.

The analytical modeling framework for detailed active composite reflector design uses SIERRA Multi-physics¹⁰ tools. These tools allow for coupled-physics simulations incorporating structural, thermal, and electrical actuation behavior.

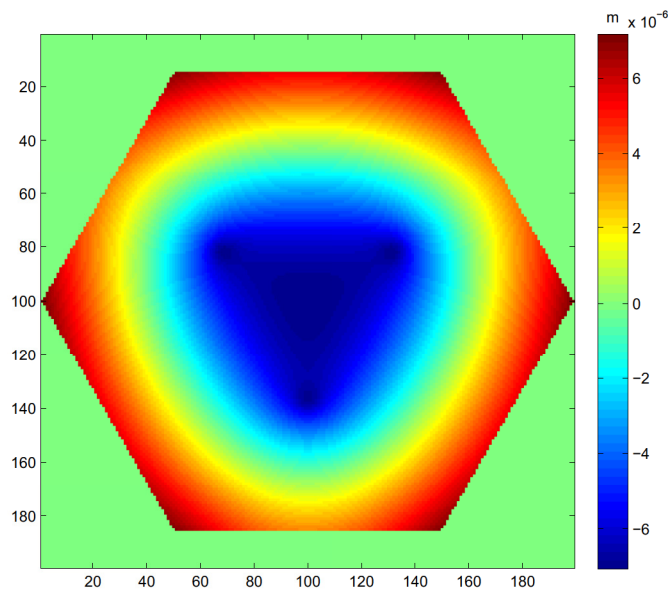


Figure 12: Modeled wavefront error sag for a gravity load along the axis of the reflector.

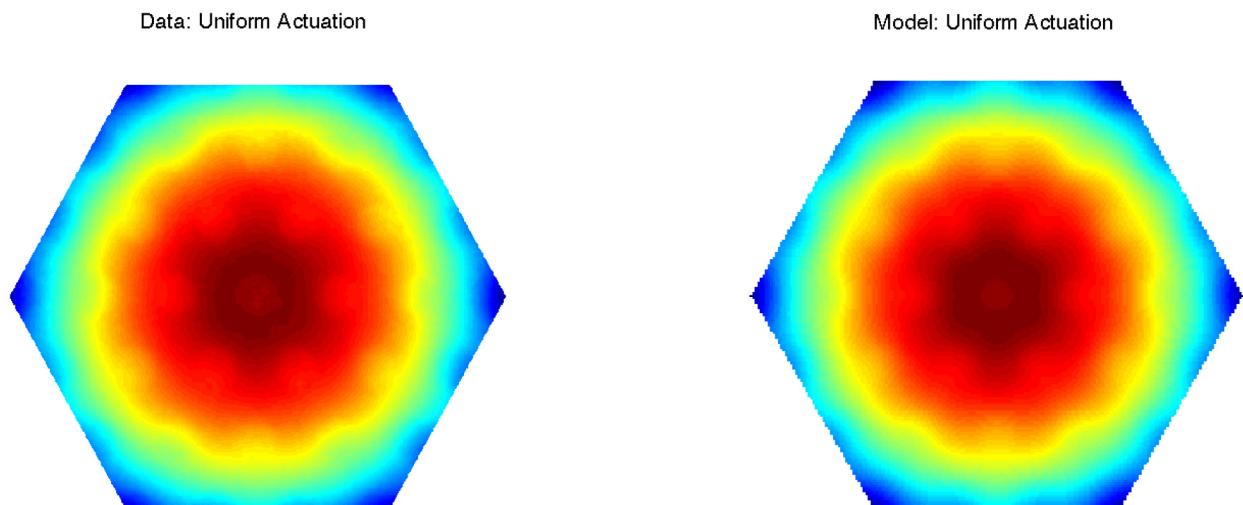
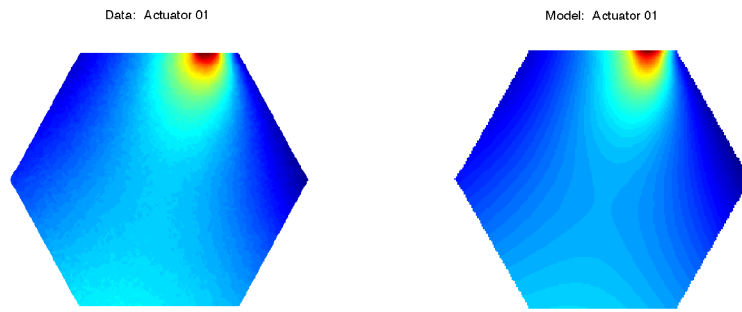
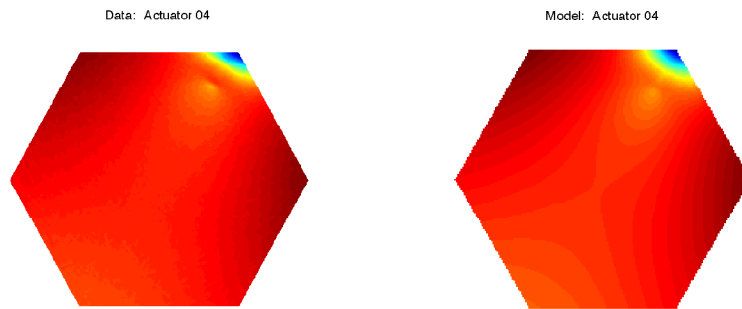


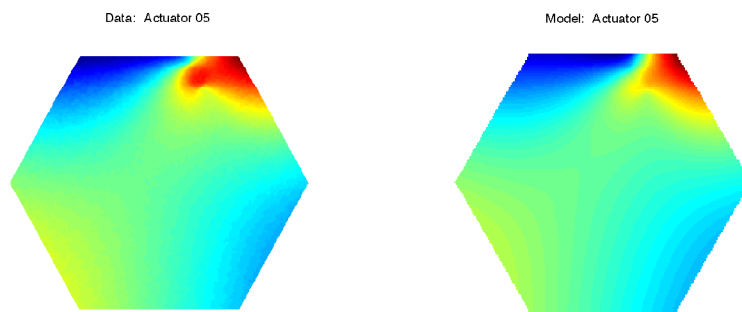
Figure 13: The model and data results for uniform actuation (normalized).



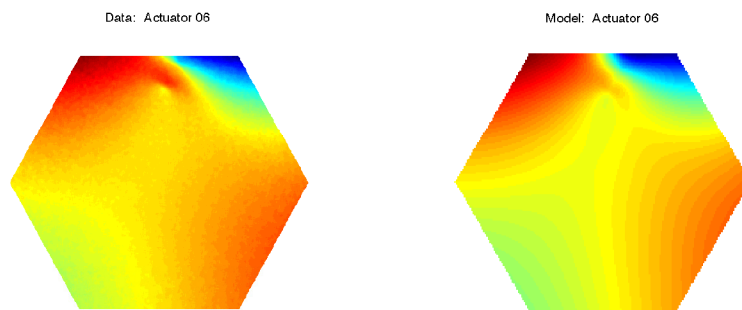
(a) Actuator 1



(b) Actuator 4



(c) Actuator 5



(d) Actuator 6

Figure 14: Sample influence function comparisons between experimental data and modeled data.

Active Flat Reflector Test Results and Model Development

The bench-scale active flat reflector (150 mm) was designed as a proof-of-concept for retrofitting optical surfaces with flat actuators to correct the surface figure. A non-uniform pattern was selected to maximize the amount of actuators, using the standard 28 x 14 mm actuator as our baseline actuator dimension. Figure 5 shows a photograph of the actuator layout and the reflector as mounted during influence function testing, and Figure 15 shows sample influence functions of each actuator superimposed on the actuator layout.

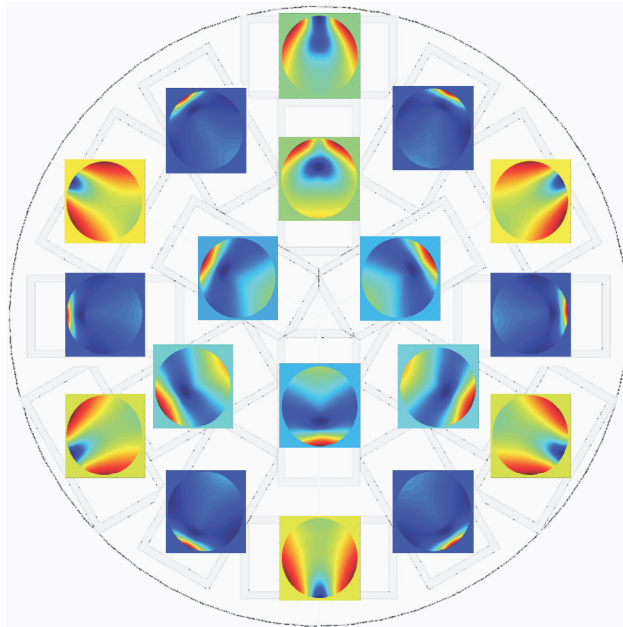


Figure 15: Active Flat Reflector actuator layout, with influence functions (taken at 700 V) superimposed on the actuator map. The glass blank is 150 mm in diameter, and the actuator active areas are 28 x 14 mm with a total actuator size of 38 x 20 mm, including electrodes and a tape border. The actuator layout has 120° symmetry.

The actuator influence functions were measured to determine actuator authority on a glass substrate. Influence functions were measured from 0-1400 V, and voltage was cycled to assess hysteresis. Voltage was applied in 200 V intervals up to 1400 V (Figure 16), then in -200 V intervals from 1300 V back to 0 V (Figure 17). In both P-V and RMS, the actuator authority shows very linear behavior, as in Figure 18.

Correcting a 6 mm thick glass substrate, with 14 x 28 mm actuators, required higher voltages than compared with the Active Composite Reflector. The current testbed does not have an 18-channel kV D/A card, so optimal correction of the surface is not possible. Some correction, however, is easily obtainable by commanding all actuators in a common circuit, as shown in Figure 19. As the actuator layout is roughly uniform, the influence of all actuators in common will approximate a spherical surface. The actuators were bonded such that in extension, they would work to counter the built-in curvature of the reflector. The glass flat has 2200 nm RMS of surface error, which is dominated by a focus term. By commanding all actuators in common at 1400 V, the RMS surface was corrected to 700 nm RMS.

Simulated results of high-voltage control show that we can improve on that result. An optical model of the system was generated from the individual influence functions to predict the corrected surface for different voltage limits. The actuators have an operating range of -500 to +1500 V, but the study was extended to investigate the numerical limits of the correction authority. Using different limit voltages (2000 and 5000 V in Figure 20), different surface quality can be predicted. The correction does not scale indefinitely, the actuator spacing is too coarse to gain much improvement past 5000 V. At 20,000 V the RMS has decreased slightly to 290 nm, which can be considered the floor of this actuator strategy.

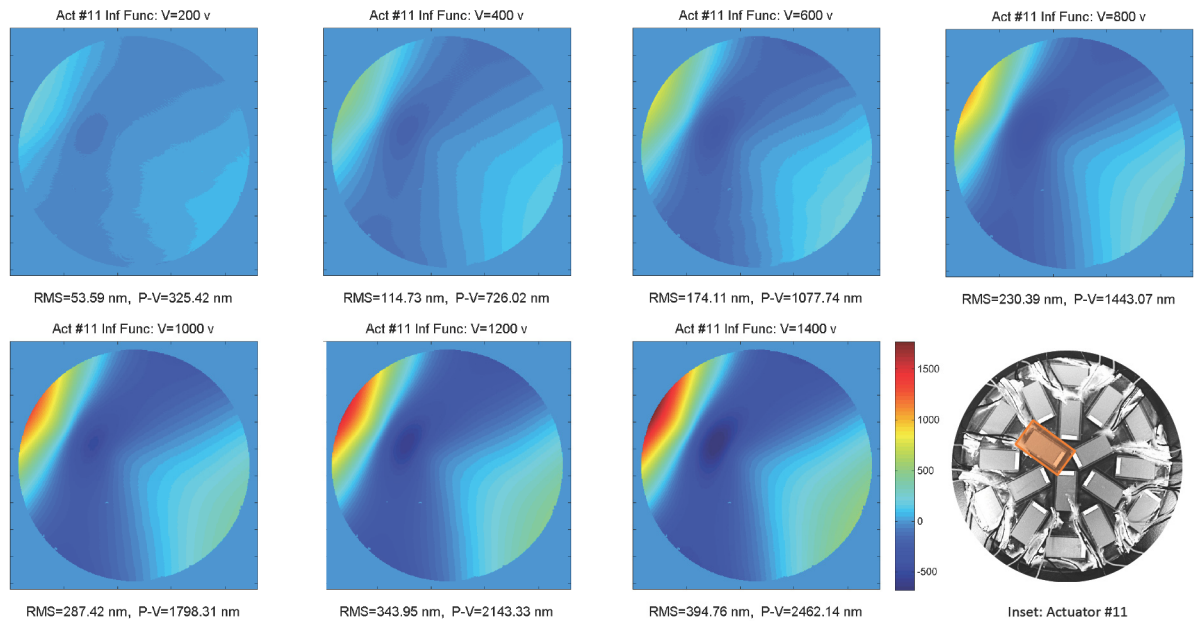


Figure 16: Active Flat Reflector influence function measurements for a selected actuator, 200 to 1400 V in 200 V increments. Influence functions measured in 100 s intervals.

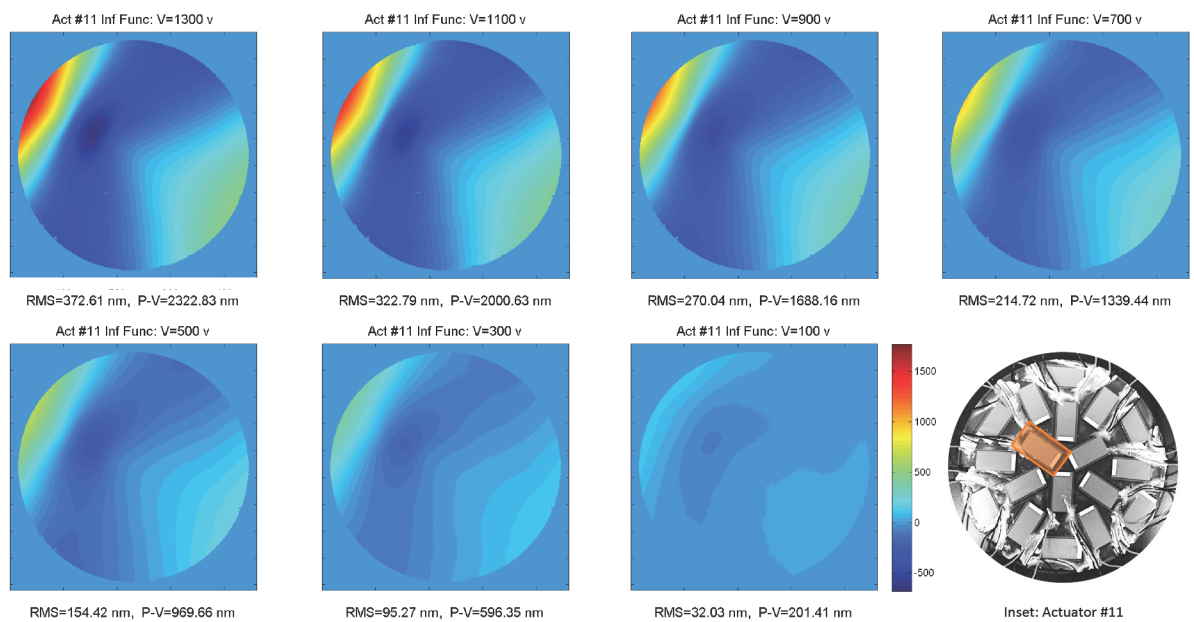


Figure 17: Active Flat Reflector influence function measurements for a selected actuator, 1300 to 100 V in -200 V increments. Influence functions measured in 100 s intervals.

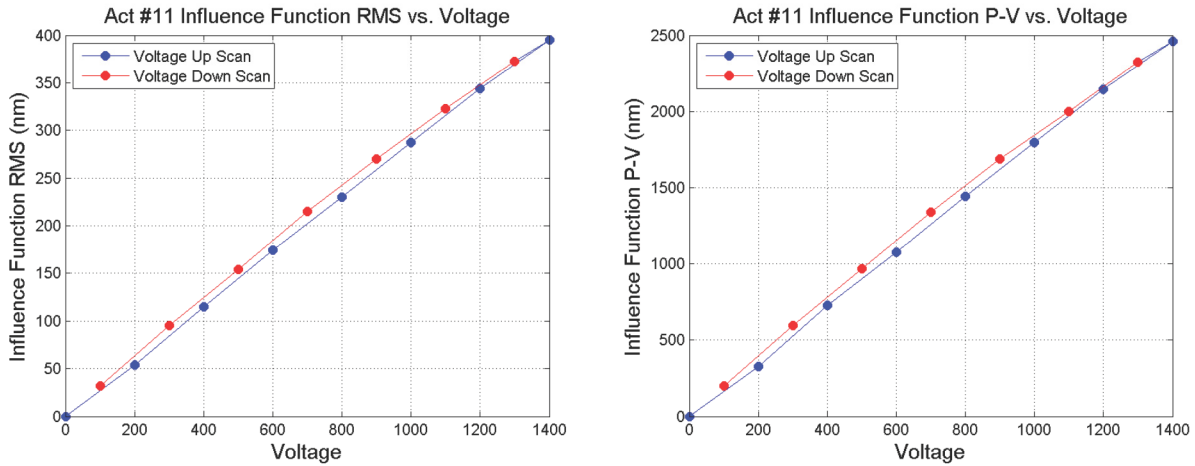


Figure 18: Active Flat Reflector influence function scan, in both RMS and P-V, shows very linear behavior and little hysteresis across one load/unload cycle. Influence functions measured in 100 s intervals. Linearity in influence function across the actuator range simplifies inverting the influence function matrix to generate a useful voltage profile for controlling deformations.

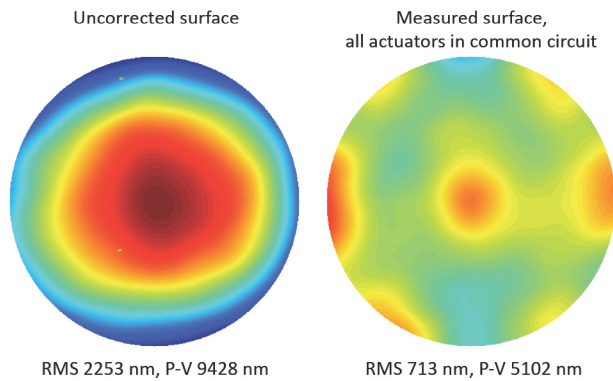


Figure 19: Active Flat Reflector, surface error and measured wavefront correction. All actuators are tied to a single high-voltage signal, effectively functioning as a single actuator, then driven to 1400 V. The as-built residual error is roughly spherical, as is the approximate shape induced by all actuators driven with a common signal. The surface can be corrected to 713 nm RMS. These results can be improved on by individually addressing each actuator with a high-voltage D/A system.

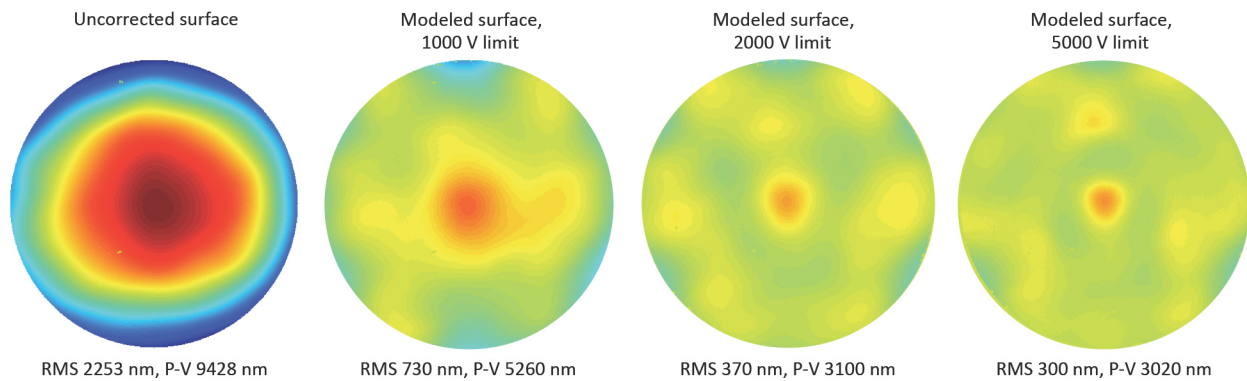


Figure 20: Active Flat Reflector, surface error and modeled wavefront correction. A best surface can be calculated using the influence functions taken at 700 V for each actuator. Assuming different voltage limits, the surface can be corrected to better than 300 nm RMS.

Acknowledgments

This research was carried out at the Jet Propulsion Laboratory, California Institute of Technology, under a contract with the National Aeronautics and Space Administration. The help and assistance provided by Phil Walkemeyer, Dan Barber, Eric Oakes, Jo Tillis, and Ari Miller is greatly appreciated.

References

- ¹Bradford, S. C., Agnes, G. S., and Wilkie, W. K., "An Active Composite Reflector System for Correcting Thermal Deformations," *AIAA 19th Adaptive Structures Conference, Denver CO, April 2011*, 2011.
- ²Bradford, S. C., Agnes, G. S., Miller, A. P., and Wilkie, W. K., "Shape Measurement and Control of an Active Panel under Thermal Loads," *26th Aerospace Testing Seminar, Long Beach, CA, March 2011*, 2011.
- ³Wilkie, W. K., Inman, D., High, J., and Williams, R., "Recent Developments in NASA Piezocomposite Actuator Technology," 2008.
- ⁴NASA, *Photo credit National Aeronautics and Space Administration, <http://www.nasa.gov>*, 2008.
- ⁵Cooper, B., Black, J., Swenson, E., and Cobb, R., "Rigidizable Inflatable Get-Away-Special Experiment (RIGEX) Space Flight Data Analysis," *AIAA 2009-2157, 50th AIAA/ASME/ASCE/AHS/ASC Structures, Structural Dynamics, and Materials Conference, 4-7 May 2009, Palm Springs, California*, 2009.
- ⁶Cofield, R. and Kasl, E., "Thermal stability of a 4 meter primary reflector for the Scanning Microwave Limb Sounder," 2010.
- ⁷Zhao, F., Ksendrov, A., Rao, S., and Kadogawa, H., "Swept-Frequency Laser Ranging Using a Calibrated Common-Path Heterodyne Interferometer," *ODIMAP V, 5th Topical Meeting on Optoelectronic Distance/Displacement Measurements and Applications, Aula de Grados, Escuela Politecnica Superior Universidad Carlos III, Madrid, Spain, October 2006*, 2006.
- ⁸Hedgepeth, J., "Critical Requirements for the Design of Large Space Structures," NASA CR 3484, 1981.
- ⁹COMSOL, *COMSOL Multiphysics: User's Guide, Version 3.5a*, 2008.
- ¹⁰Sandia, *SIERRA Mechanics*, sandia.gov, 2011.
- ¹¹Bradford, S. C., Agnes, G. S., and Wilkie, W. K., "Active Thermal Distortion Compensation for Lightweight Composite Reflectors," R&TD Year 1 Report, JPL, 2010.